

Technical Manual for the SAM Solar Water Heating Model

Nicholas DiOrio, Craig Christensen, Jay Burch, Aron Dobos

March 31, 2014

Abstract

This manual documents the methodology and validation of the solar water heating performance model used in the NREL System Advisor Model (SAM) software. The model estimates the energy savings of using solar water heating system relative to a conventional water heater using a thermodynamic energy balance formulation. Simplifications in the treatment of stratified temperatures in storage tanks relative to more complex models available in tools such as TRNSYS yield very fast runtimes and good agreement on an hourly, monthly, and annual basis with much more detailed and validated simulations.

Keywords: *solar water heating, thermodynamic model, System Advisor Model, systems modeling*

Contents

1	Overview	3
2	Mixed-Tank Mode	3
2.1	Heat Sources	3
2.1.1	Useful energy delivered	3
2.1.2	Tank Heat Loss to Room	5
2.1.3	First Law of Thermodynamics	6
2.2	Time-Marching Method	7
2.2.1	Implicit Euler Model	7
3	Stratified-Tank Mode	8
3.1	Assumptions	8
3.2	Energy Modeling Overview	9
3.2.1	Room loss	9
3.3	Volumes	9
3.4	Hot Water	9
3.5	Cold Water	10
4	Additional Relations	11
4.1	Transmitted Irradiance	11
4.2	Energy Delivered	12
5	Validation	13
5.1	Comparison Model	13
5.2	Combined Behavior	13
5.3	Mixed Comparison	13
5.4	Stratified Comparison: Hot	15
5.5	Stratified Comparison: Cold	16
5.6	Energy Saved	16
5.7	Annual Percent Differences	16
6	Transitioning From SAM-TRNSYS	18
6.1	SAM-TRNSYS Model	18
6.2	Motivation for replacement	18
6.3	Simple Model Comparison	19
6.3.1	Tank Temperature	19
6.3.2	Energy Saved	19
6.3.3	Annual Percent Differences	20
7	Conclusion	22
8	Nomenclature	23
	References	23

1 Overview

Due to the complexity gap between the solar-water heating models in TRNSYS [1] and fChart, there is interest in deriving and using a model which provides more flexibility than the simple model in fChart without having to deal with the challenges of modeling with TRNSYS. One idea for a model [2] is to assume that the solar water heater undergoes two distinct modes. The first of these modes is during solar charging, where the storage tank is assumed to be one mixed node. The second of these modes is during discharging, where the storage tank is assumed to be two variable-volume nodes, one of hot water, and one of incoming cold water from the mains [3].

The primary purpose of this paper will be to fully explain the derivation of the tank temperatures during both modes. This simple dual-mode model will be compared to a detailed 100 node TRNSYS model developed as a validation tool. The simple dual-model model will also be compared to a two-tank TRNSYS model previously used as the solar water heating tool in the System Advisor Model (SAM). The simple model has replaced the SAM-TRNSYS model in versions of SAM newer than 2013.1.15.

The nomenclature followed for this paper will closely follow that from [2]. Of note is that this paper will use C_p to represent specific heat, though for liquids the distinction between constant volume and constant pressure specific heats is not necessary [4].

2 Mixed-Tank Mode

The system architecture consists of a solar collector which has a working fluid running through it, as in Figure 1. When the fluid has gone through the collector, it enters a heat exchanger, where it transfers heat to cooler water. The water heats up and is stored in a tank. There are also pumps to force circulation of the working fluid and water. The tank is considered mixed during hours where there is solar collection.

2.1 Heat Sources

If we examine the tank, it is easy to define a few quantities of heat transfer in addition to energy storage. There will be heat transfer to the room, heat transfer from the tank to the cold incoming water, and energy received from the solar collector minus any losses from the collector to the outside, which when combined, is called \dot{Q}_{useful} . This paper will use relations from [5] to develop the simple model based on this system.

2.1.1 Useful energy delivered

The useful energy delivered to the water tank is the energy received by the collector minus losses from the collector to the surroundings. The energy gained across the collector is:

$$\dot{Q}_{useful} = \dot{m}C_p[T_{f,o} - T_{f,i}] \quad (2.1.1)$$

Where f,i refers to "fluid inlet" and f,o to "fluid outlet". The temperature rise across the collector $T_{f,o} - T_{f,i}$ depends on the incident radiation. The minimum heat loss from the collector to the outside would occur if the whole collector were at the fluid inlet temperature. This is because the fluid inlet is the coldest fluid temperature in the collector, and colder temperatures

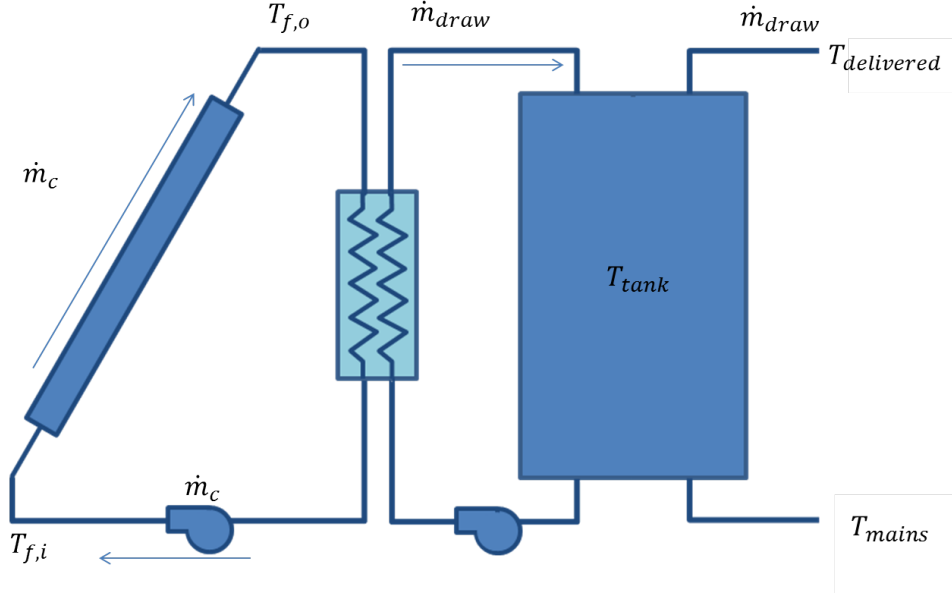


Figure 1. Solar Water Heating System

mean lower gradients between the collector and the outside. We can express this minimum loss as:

$$\dot{Q}_{min,loss} = A_c U_L (T_{f,i} - T_o) \quad (2.1.2)$$

Where U_L is the overall collector heat loss coefficient. The derivation of this coefficient is fairly involved [5], and will not be presented. For a single-cover collector, U_L depends on the convection coefficient between the absorbing plate and glass cover, the radiation coefficient from the plate to the cover, and the radiation coefficient for the cover to the air. Representative values of U_L are tabulated for various collector configurations [5]. Using the minimum loss, we can define the maximum gain across the solar collector as:

$$\begin{aligned} \dot{Q}_{max,collected} &= \dot{Q}_{solar} - \dot{Q}_{min,loss} \\ &= A_c [I\tau\alpha - U_L(\bar{T}_t - T_o)]; \end{aligned} \quad (2.1.3)$$

In this equation, I is the solar insolation, and $\tau\alpha$ is the transmittance-absorbance product which accounts for optical losses. Also note that the collector inlet fluid temperature has been changed to the mean-tank temperature to reflect that water entering the collector during the collection mode is coming from the tank. It is now useful to define a modifier relating the useful energy gain to the maximum possible gain:

$$\begin{aligned} \dot{Q}_{useful} &= F_R \dot{Q}_{max,collected} \\ &= F_R A_c [I\tau\alpha - U_L(T_{f,i} - T_o)] \\ &= F_R A_c [I\tau\alpha - U_L(\bar{T}_t - T_o)] \end{aligned} \quad (2.1.4)$$

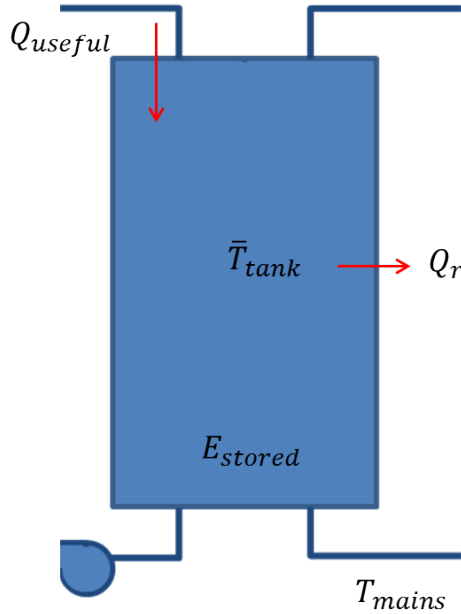


Figure 2. Energy Balance

The reason this is desirable is because we want our equation for useful energy to include the temperature of the fluid entering the collector. Interestingly the definitive reference text on this topic [5] says: "This is the most important equation in this book". But, what is F_R ? This term is called the collector heat removal factor and is derived by taking (2.1.4) and substituting other expressions for the temperature terms and manipulating. The process is again involved, but a summary of the steps is to derive the useful heat flux per unit length between the tubes within the collector, derive the useful heat flux per unit length in the flow direction within the tubes, and apply these relations to (2.1.4). The term is also updated to account for the heat exchanger, pipes, and flow rate. These adjustments can be found on pages 427, 430, and 307 of [5] respectively.

2.1.2 Tank Heat Loss to Room

Referring to Figure 2, it is assumed that the storage tank is inside a room either in a house or some storage structure. The room is likely at a different temperature than the mean tank temperature, and the tank is not perfectly insulated, thus heat transfer will occur. The type of heat transfer which will occur in this case is assumed to be a combination of convection loss between moving tank water and the tank walls, conduction loss through the tank walls, radiation from the tank walls to the room, and convection between the room and tank. An overall tank heat loss coefficient U is used, so that this complicated thermal circuit can be represented by a resistance between two nodes. Composite system heat transfer in this form can be represented by an expression analogous to Newton's Law of Cooling: [6]:

$$\dot{Q}_r = UA_t(\bar{T}_t - T_r) \quad (2.1.5)$$

Of note is that composite systems of this form use the end-points of the thermal circuit to compute the temperature difference, in this case, the mean tank temperature and the room temperature. The value of U either must be calculated based on physical properties and knowledge of temperatures or by choosing a representative value based on previous experience.

2.1.3 First Law of Thermodynamics

As cold water enters the bottom of the tank, the enthalpy of the water in the tank decreases. Recall the conservation of energy for an open system with no kinetic or potential energy changes [6]:

$$\frac{dE_{cv}}{dt} = \dot{Q}_{cv} - \dot{W}_{cv} + \sum_i \dot{m}_i h_i - \sum_e \dot{m}_e h_e \quad (2.1.6)$$

There is no source of work in the tank, so that term goes to zero. We also make the assumption that the mass flow rate entering the tank is the same as leaving the tank, allowing us to rewrite this as:

$$\frac{dE_{cv}}{dt} = \dot{Q}_{cv} + \dot{m}_{draw}[h_i - h_e] \quad (2.1.7)$$

We can exploit basic thermodynamic relations for liquids to further simplify the enthalpy expression:

$$h_i - h_e = C_p[T_i - T_e] \quad (2.1.8)$$

Where the inlet temperature is determined from the cold water entering the tank, and the exit temperature is assumed to be the mean tank temperature such that:

$$h_i - h_e = C_p[T_{mains} - \bar{T}_t]; \quad (2.1.9)$$

This means we can write (2.1.6) as:

$$\frac{dE_{cv}}{dt} = \dot{Q}_{cv} - \dot{m}_{draw}C_p[\bar{T}_t - T_{mains}] \quad (2.1.10)$$

We assume that the energy of the control volume is the internal energy of the water, such that:

$$E_{cv} = \rho V_t C_p \bar{T}_t \quad (2.1.11)$$

Then, we can write:

$$\frac{dT_t}{dt} = \frac{\dot{Q}_{cv} - \dot{m}_{draw}C_p[\bar{T}_t - T_{mains}]}{\rho V_t C_p} \quad (2.1.12)$$

Where we have made the assumption that the density, specific heat, and volume of the water in the tank are constant. Clearly this is a linear, first-order differential equation of the form:

$$\frac{dT}{dt} = f(t, T) \quad (2.1.13)$$

2.2 Time-Marching Method

2.2.1 Implicit Euler Model

We can choose from a vast selection of time-marching methods [7], but for simplicity and stability purposes will approximate all differential equations using the implicit-Euler method. Of note, this is only a first-order accurate method, but because of the many simplification steps we have taken, it doesn't necessarily make sense to try and achieve higher-order approximations.

$$T_{i+1} = T_i + \Delta t f(t_{i+1}, T_{i+1}) \quad (2.2.1)$$

The implicit-Euler method is first-order accurate in time, and unconditionally stable, but as with all implicit methods, requires solving a linear system at each time step. Applying this numerical method to (2.1.12), we get:

$$\bar{T}_t = T_{t,p} + \Delta t \left(\frac{\dot{Q}_{cv} - \dot{m}_{draw} C_p [\bar{T}_t - T_{mains}]}{\rho V_t C_p} \right) \quad (2.2.2)$$

The heat transfer rate is derived by examining Figure 2 and summing each heat term by assuming heat coming in is positive and heat going out is negative:

$$\dot{Q}_{cv} = \dot{Q}_{useful} - \dot{Q}_{room} \quad (2.2.3)$$

Plugging in the expression for the heat transfer:

$$(\bar{T}_t - T_{t,p}) = \frac{\dot{Q}_{useful} \Delta t - \dot{Q}_{room} \Delta t - \dot{m}_{draw} C_p [\bar{T}_t - T_{mains}] \Delta t}{\rho V_t C_p} \quad (2.2.4)$$

This is the model equation for the implicit method. Plugging in the expressions for each heat term, we get:

$$(\bar{T}_t - T_{t,p}) = \frac{A_c F_R (\tau \alpha I - U_L [\bar{T}_t - T_o]) \Delta t - U A_t [\bar{T}_t - T_r] \Delta t - \dot{m}_{draw} C_p [\bar{T}_t - T_{mains}] \Delta t}{\rho V_t C_p}$$

This is the equation we must solve at every time step to map the evolution of temperature. Since the model we have derived is linear, it is possible to solve for a closed form solution for \bar{T}_t . Expand all the terms in (2.2.4), bring all \bar{T}_t terms to one side, factor, and divide through to get:

$$\bar{T}_t = \frac{T_{t,p}\rho V_t C_p + (A_c F_R [\tau \alpha I + U_L T_o] + U A_t T_r + \dot{m}_{draw} C_p T_{mains}) \Delta t}{\rho V_t C_p + (A_c F_R U_L + U A_t + \dot{m}_{draw} C_p) \Delta t} \quad (2.2.5)$$

A simple first step towards validating this model is to check that the dimensions are consistent. Going through this exercise, one should find that each side equates to a unit of temperature. Writing the dimensions for the terms:

$$\begin{aligned} [K] &= \frac{[K kg \frac{J}{kg K}] + [m^2 \frac{Ws}{m^2}] + [m^2 \frac{Ws}{m^2 K} K] + [\frac{Ws}{m^2 K} m^2 K] + \frac{kg}{s} \frac{J}{kg K} K s}{[kg \frac{J}{kg K}] + [m^2 \frac{Ws}{m^2 K}] + [\frac{Ws}{m^2 K} m^2]} \\ &= [\frac{J}{K}] \\ &= [K] \end{aligned} \quad (2.2.6)$$

This model is dimensionally consistent. Note, the units for solar radiation is watts per meter squared.

3 Stratified-Tank Mode

The second mode is during discharging, where the storage tank is assumed to be two variable-volume nodes, one of hot water, and one of incoming cold water from the mains [3]. The primary interest of this section will be to fully explain the derivation of the tank temperatures during the stratified mode, using the following for an overview of the water tank shown in Figure 3.

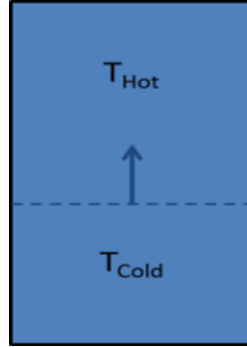


Figure 3. Stratified Tank

3.1 Assumptions

There a couple of assumptions fundamental to this mode. The first is that no conduction occurs between the hot and cold water in the tank. Clearly, this is not physically correct; nevertheless a back-of-the-envelope calculation suggests that the conduction is only about five percent of the total energy transfer for a typical case. It would not be difficult to add conduction to the model in the future.

The second assumption is that when heat is exiting the system, it is assumed to be negative, whereas it is positive if entering the system. This is the opposite of the work convention, which assumes work done by the system is positive.

3.2 Energy Modeling Overview

If we examine the tank we only have heat transfer to the room from the hot water in the tank, and heat transfer to the cold water from the room. We have assumed no heat conduction from the hot water to cold water for this simple model.

3.2.1 Room loss

Heat transfer occurs to the room in the same manner as described for the mixed-tank mode, except there are two nodes to consider:

$$\dot{Q}_{r,cold} = UA_{cold}[T_r - T_{cold}] \quad (3.2.1)$$

$$\dot{Q}_{r,hot} = UA_{hot}[T_r - T_{hot}] \quad (3.2.2)$$

3.3 Volumes

During discharging, the volume of hot water decreases as users draw it. Cold water enters the bottom of the tank from the mains to replenish the water. It is simple to model the volume of the hot and cold water as:

$$V_{hot} = V_{hot,p} - \frac{\dot{m}_{draw}\Delta t}{\rho} \quad (3.3.1)$$

$$V_{cold} = V_t - V_{hot} \quad (3.3.2)$$

Calculating these volumes is critical at every time step, because they allow the calculation of mass in each node. Of note is that the initial condition when switching from collection mode is $V_{hot} = V_t$ and $V_{cold} = 0$. Mass is calculated as $m = \rho V$.

3.4 Hot Water

Since the volume and hence mass of hot water varies dynamically, we must take this into consideration when formulating the energy balance [4]. The left hand side of the energy balance takes the form:

$$\frac{d(m_{hot}C_p T_{hot})}{dt} = m_{hot}C_p \frac{dT_{hot}}{dt} + T_{hot}C_p \frac{dm_{hot}}{dt} \quad (3.4.1)$$

Where it is apparent that the product rule applies due to both the temperature and mass of the hot water varying in time. The mass flow rate of hot water exiting the control volume is equal to the amount of water being drawn by the user. This means that the mass flow rate out of the hot node is negative.

$$\dot{m}_{hot} = -\dot{m}_{draw} \quad (3.4.2)$$

Assuming perfectly stratified behavior there will be no mass entering the hot control volume. The energy balance takes the form:

$$-\dot{m}_{draw}C_pT_{hot} + m_{hot}C_p\dot{T}_{hot} = \dot{Q}_{r,hot} + \dot{m}_{draw}[-h_e] \quad (3.4.3)$$

$$m_{hot}C_p\dot{T}_{hot} = \dot{Q}_{r,hot} - \dot{m}_{draw}C_pT_{hot} + \dot{m}_{draw}C_pT_{hot} \quad (3.4.4)$$

$$\dot{T}_{hot} = \frac{-UA_{hot}[T_{hot} - T_r]}{m_{hot}C_p} \quad (3.4.5)$$

Implicitly approximating the differential equation results in:

$$T_{hot} = \frac{T_{hot,p}m_{hot}C_p + \Delta tUA_{hot}T_r}{m_{hot}C_p + \Delta tUA_{hot}} \quad (3.4.6)$$

A_{hot} is simply the outer surface area of the portion of the tank that contains hot water, which includes the top surface area.

$$H_{hot} = \frac{V_{hot,p}}{\pi r_t^2} \quad (3.4.7)$$

$$A_{hot} = \pi r_t^2 + 2\pi r_t H_{hot} \quad (3.4.8)$$

Where H_{hot} is the variable height of hot water.

3.5 Cold Water

As with the hot water we need to account for the variable volume of the cold node:

$$\frac{d(m_{cold}C_pT_{cold})}{dt} = m_{cold}C_p\frac{dT_{cold}}{dt} + TC_p\frac{dm_{cold}}{dt} \quad (3.5.1)$$

The mass flow rate of the cold water should be roughly equal to the amount of water entering the system, which has been approximated as equal to the user draw:

$$\dot{m}_{cold} = \dot{m}_{draw} \quad (3.5.2)$$

The energy balance takes the form:

$$\dot{m}_{draw}C_pT_{cold} + m_{cold}C_p\dot{T}_{cold} = UA_{cold}(T_r - T_{cold}) + \dot{m}_{draw}h_i \quad (3.5.3)$$

$$m_{cold}C_p\dot{T}_{cold} = UA_{cold}(T_r - T_{cold}) + \dot{m}C_p(T_{mains} - T_{cold}) \quad (3.5.4)$$

$$\dot{T}_{cold} = \frac{UA_{cold}(T_r - T_{cold}) + \dot{m}C_p(T_{mains} - T_{cold})}{m_{cold}C_p} \quad (3.5.5)$$

Where:

$$H_{cold} = \frac{V_{cold,p}}{\pi r_t^2} \quad (3.5.6)$$

$$A_{cold} = \pi r_t^2 + 2\pi r_t H_{cold} \quad (3.5.7)$$

Applying implicit Euler:

$$T_{cold} = \frac{T_{cold,p} m_{cold} C_p + \Delta t (U A_{cold} T_r + \dot{m}_{draw} C_p T_{mains})}{m_{cold} C_p + \Delta t (U A_{cold} + \dot{m}_{draw} C_p)} \quad (3.5.8)$$

4 Additional Relations

The unique aspects have been presented; however, there are additional relations that are important to present.

4.1 Transmitted Irradiance

The incident irradiation is computed depending on the sky-model input by the user. The sky models available are isotropic, HDKR, and Perez, which are summarized in [5] on pg. 96, or in the original papers [8], [9]. The calculation of incident irradiation is the sum of beam, diffuse, and ground reflected radiation:

$$I_i = I_b + I_d + I_g \quad (4.1.1)$$

Where i, b, d, g stand for "incident", "beam", "diffuse", and "ground" respectively. The amount of irradiation transmitted is dependent on the angle of incidence. Each component of radiation must be modified as:

$$I_t = K_{\tau\alpha,b} I_b + K_{\tau\alpha,d} I_d + K_{\tau\alpha,g} I_g \quad (4.1.2)$$

Where the $K_{\tau\alpha}$ terms are known as incidence angle modifiers. These modifiers are values between 0 and 1 which reflect how much radiation is transmitted at a certain angle relative to how much radiation would be transmitted when the radiation is directly normal to the collector [5]. A general expression is commonly used to estimate the modifiers at angles less than or equal to 60°.

$$K_{\tau\alpha} = 1 - b_o \left(\frac{1}{\cos(\theta) - 1} \right) \quad (4.1.3)$$

Where b_o is called the incidence angle modifier coefficient. For the beam component, the angle in (4.1.3) is simply the angle of incidence. For the diffuse and ground components, the angles used (in degrees) are:

$$\theta_d = 59.7 - 0.1388\beta + 0.001497\beta^2 \quad (4.1.4)$$

$$\theta_g = 90 - 0.5788\beta + 0.002693\beta^2 \quad (4.1.5)$$

Where β is the collector slope measured in radians. At angles larger than 60° , the approximation of (4.1.3) breaks down as the relation between $K_{\tau\alpha}$ and incidence angle becomes more non-linear [5]. For angles between $60 - 90^\circ$, the incidence angle modifiers are computed as:

$$K_{\tau\alpha} = (1 - b_o)(\theta - 90) \frac{\pi}{180} \quad (4.1.6)$$

This is a simple straight line which has the property of being equal to 0 when $\theta = 90^\circ$ and equal to $1 - b_o$ when $\theta = 60^\circ$.

4.2 Energy Delivered

The energy delivered by the solar collection process is computed at the output of the solar storage tank as:

$$Q_{delivered} = \dot{m}_{draw} C_p (T_{deliv} - T_{mains}) \quad (4.2.1)$$

The auxiliary energy required to bring the water to the set temperature after solar collection is computed as:

$$Q_{aux} = \eta_{aux} \dot{m}_{draw} C_p (T_{set} - T_{deliv}) \quad (4.2.2)$$

Where η_{aux} is the efficiency of the auxiliary tank and is assumed to equal one for an electric source. The amount of auxiliary energy that would be required if solar water heating was not used would be:

$$Q_{aux,only} = \eta_{aux} \dot{m}_{draw} C_p (T_{set} - T_{mains}) \quad (4.2.3)$$

The amount of energy saved is how much less auxiliary was required due to solar water heating minus the amount of pump power required to drive the collector and tank flow:

$$Q_{saved} = Q_{aux,only} - Q_{aux} - P_{pump} \quad (4.2.4)$$

The solar fraction, which is a ratio of how much energy is saved by solar heating to how much energy total is required can be approximated as:

$$F_{net} = \frac{Q_{saved}}{Q_{aux,only}} \quad (4.2.5)$$

This representation includes the effect of parasitic power to the pump.

5 Validation

5.1 Comparison Model

A detailed TRNSYS model developed to validate this dual-mode configuration was used to generate a baseline of comparison. Temperature comparisons from each mode of operation will be presented, in addition to other quantities of interest such as energy saved. Parameters used for the comparison are shown in Table 1.

Table 1. Simple to TRNSYS comparison parameters

Variable	Value
Location	Denver Int. Airport
Albedo	0.2
Irradiance Model	Isotropic
Irradiance Inputs	Beam and Diffuse
Collector \dot{m}	$0.06 \frac{kg}{s}$
Collector Area	$4 m^2$
Collector Slope	30°
Collector Azimuth	South
$F_R(\tau\alpha)$	0.7
$F_R U_L$	$3 \frac{W}{m^2 C}$
Incidence Angle Modifier	0.2
Heat Exchanger Effectiveness	0.75
Pump Power	30 W
Pump Efficiency	1
Room Temperature	$20^\circ C$
Set Temperature	$55^\circ C$
Tank Volume	$0.3 m^3$
Tank U	$1 \frac{W}{m^2 C}$

5.2 Combined Behavior

With a two-mode model, it is important to verify that both modes are turning on and behaving as expected. A simple validation is to plot the mixed-tank temperature during charging, and the hot and cold node temperatures during stratified discharging. As Figure 4 shows, the tank temperature increases throughout the day as collection gathers solar energy and delivers it to the tank water. Once the sun goes down and collection stops, the mode switches to stratified discharging, where the hot volume decreases and cold volume increases, causing the hot node temperature to decrease until morning comes and charging begins again.

5.3 Mixed Comparison

The tank-temperature for the different models are shown in Figure 5. The detailed TRNSYS model follow the same trend, while the SAM model does not. Of note is that only the data where the simple model is in mixed mode are shown.

What is notable about hours 4024-4072 is that the simple model very closely tracks the detailed TRNSYS model and the older SAM TRNSYS model during charging, which is the

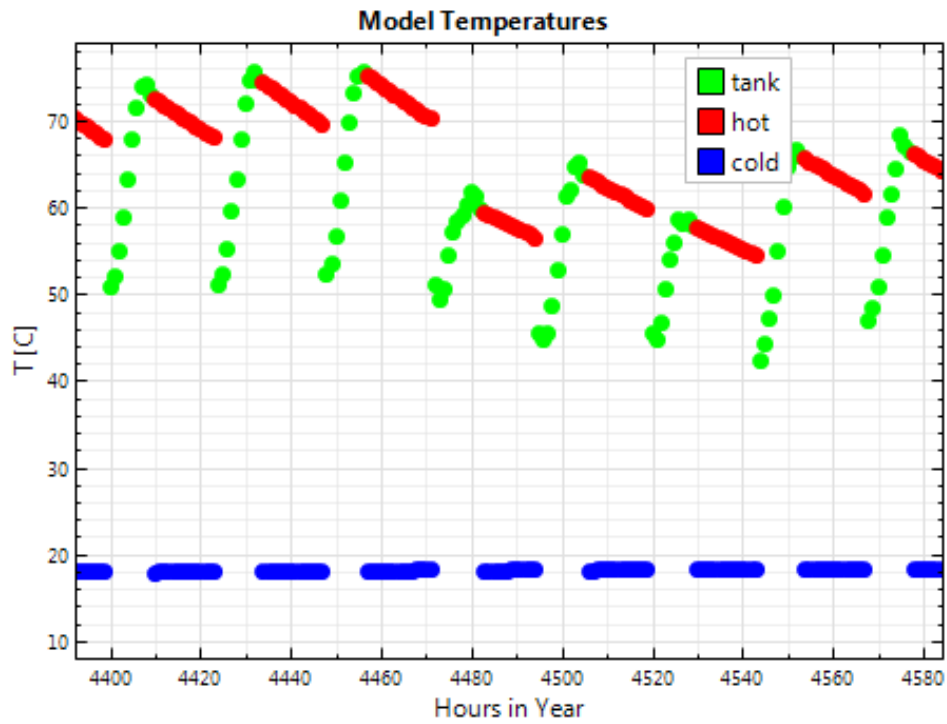


Figure 4. Simple Dual-Mode Behavior

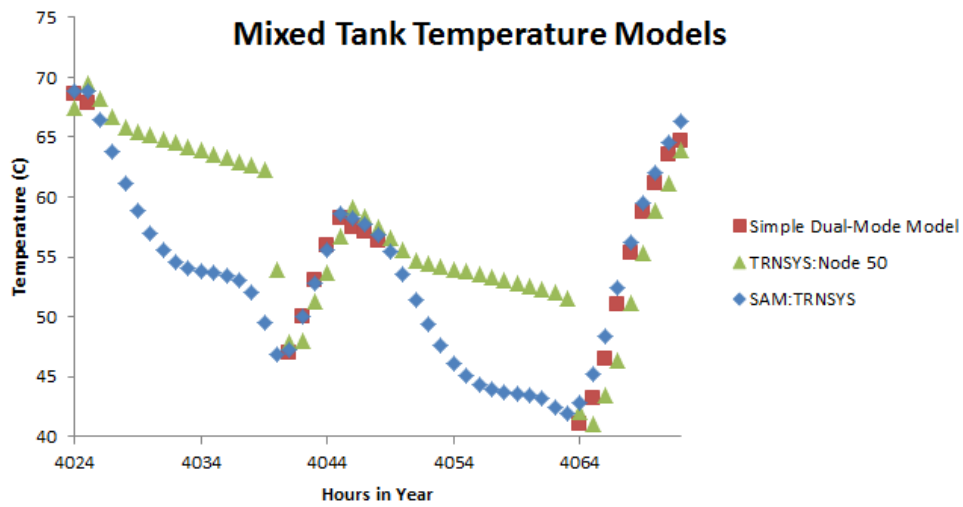


Figure 5. Tank Temperature Comparisons

intended range of use. Daily averaged data for the whole year against the detailed TRNSYS model provides a more complete comparison as seen in Figure 6.

The simple model appears to track the mean tank temperature daily average well.

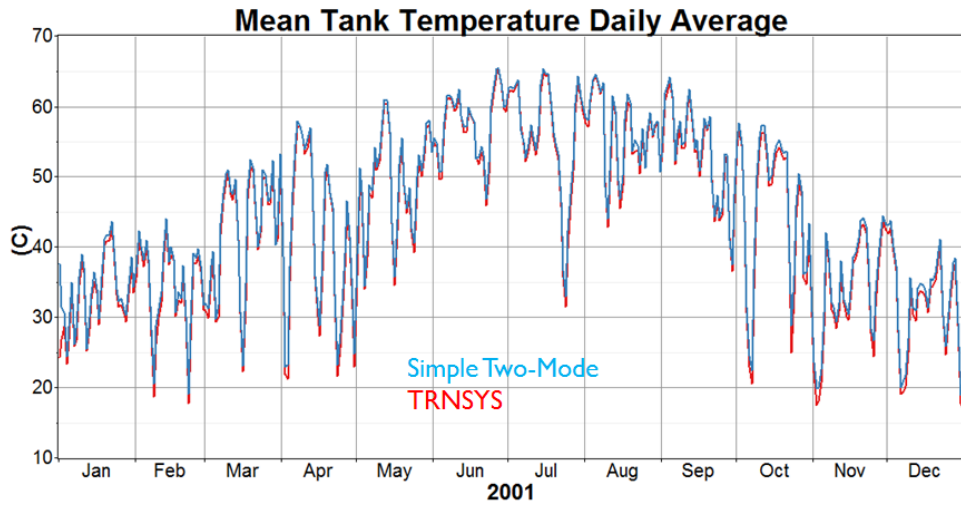


Figure 6. Tank Temperature Comparison

5.4 Stratified Comparison: Hot

In Figure 7, the daily average hot temperature over the whole year is considered.

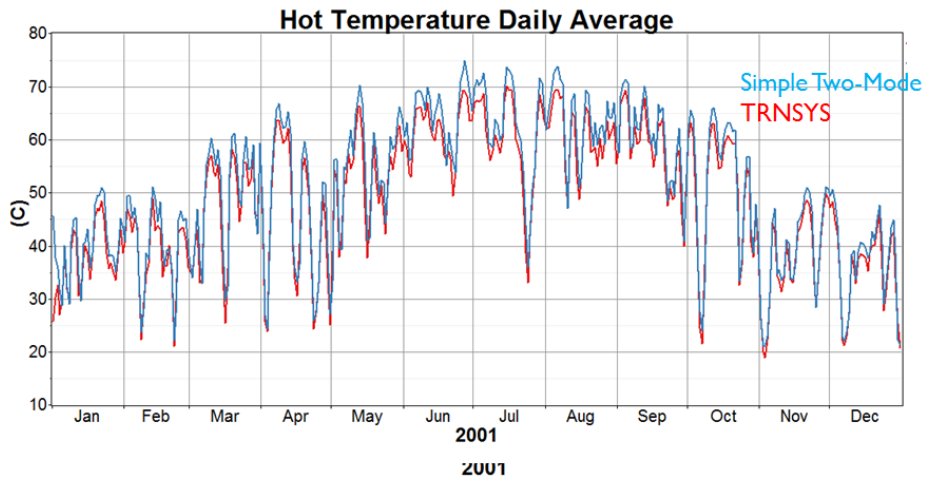


Figure 7. Hot Comparison

It appears that on average, the simple-model slightly over-predicts the hot-node temperature. Again, consider that the daily average mixes together charging and discharging modes and is thus not necessarily a true reflection of the accuracy of an individual mode. The primary point of the graph is that general daily trends are followed. The next comparison to consider is the cold-node temperature.

5.5 Stratified Comparison: Cold

To get a sense of the entire year, we can again consider the daily average cold temperature compared to the TRNSYS result in Figure 8.

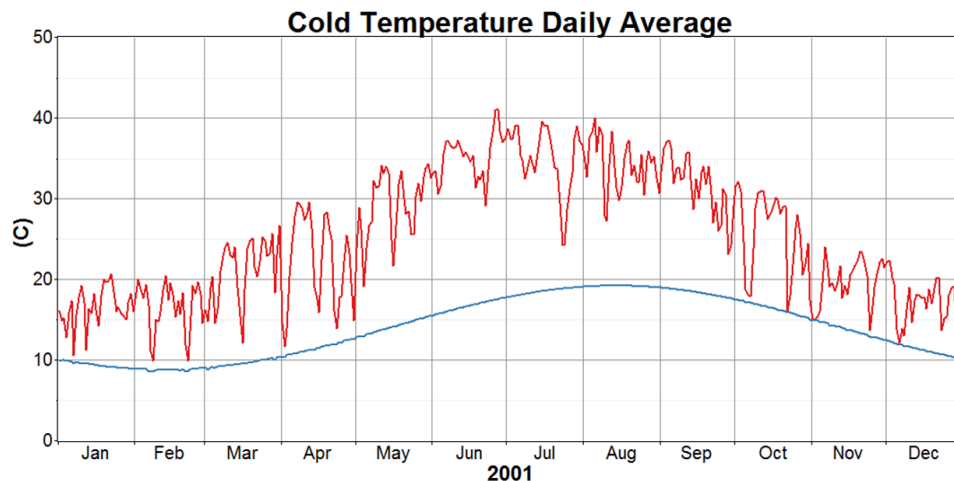


Figure 8. Cold Comparison: Red = TRNSYS, Blue = Simple Dual Mode

Cold temperatures are still output to provide a full 8760 length set of data, but during the charging mode, the cold-node temperature is unimportant. The only comparison that matters is when the discharging mode takes effect. During this period, the cold prediction matches well. Because of the aggregate nature of a daily average and the large jumps in node temperatures during charging, the daily average comparison does not accurately reflect the benefit of the simple model prediction.

5.6 Energy Saved

Results have been shown detailing temperature comparisons between models. Next, we will turn to the most important aspect of a solar water heater: how much energy is saved by using it. First we compare against the detailed TRNSYS result using daily averages in Figure 9.

It appears that the simple model compares well against the detailed simulation for daily average energy saved. Figure 10 illustrates a typical day for each month for both the simple dual-mode and detailed TRNSYS models.

The typical day profiles are reassuring, since they illustrate the simple model can track the daily trend in energy savings predicted by the detailed TRNSYS model. A different comparison can be done via a scatter plot, as seen in Figure 11.

The scatter plot reveals that the simple mode predicts slightly lower energy saved from hour to hour throughout the year. While the simple model does not perfectly predict savings, it is clear from all of the energy savings plots that general trends and magnitudes are tracked.

5.7 Annual Percent Differences

To compare performance on an annual basis, the percent differences between total annual quantities can be compared using:

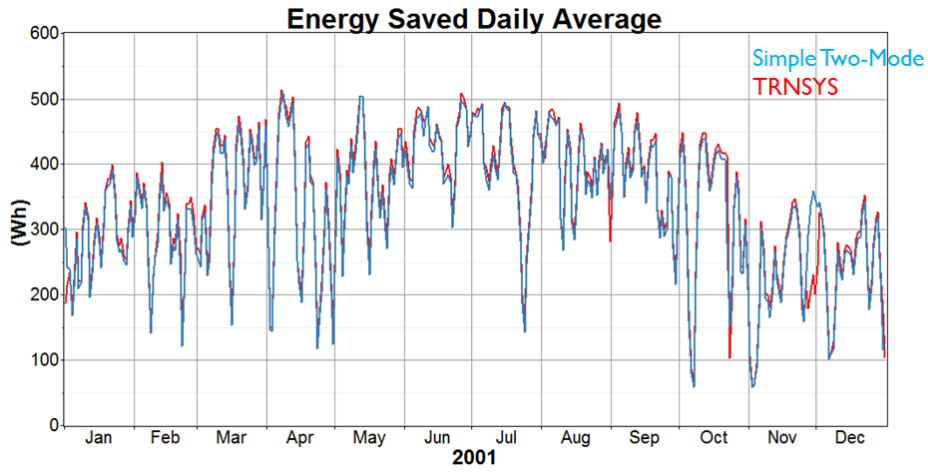


Figure 9. Energy Saved Comparison

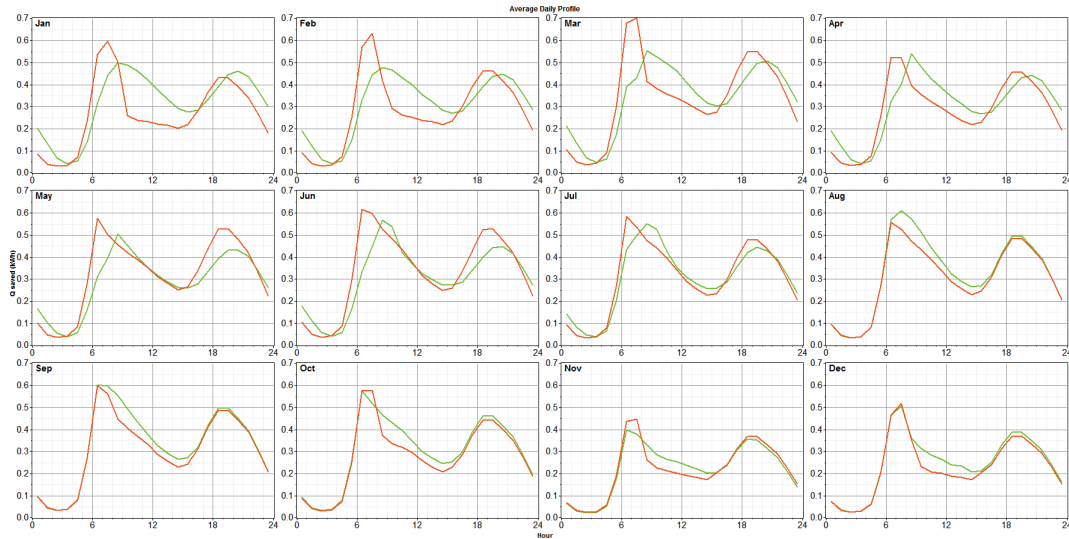


Figure 10. Typical Day Profile: Green = Detailed TRNSYS, Red = Simple Dual Mode

$$p = \frac{TRNSYS - Simple}{TRNSYS} * 100 \tag{5.7.1}$$

Table 2 shows the results.

Table 2. Annual Percent Differences

Location	Irradiance	Collected Energy	Aux. Energy	Energy Saved
Denver Airport	0.36	-3.52	8.15	-3.29

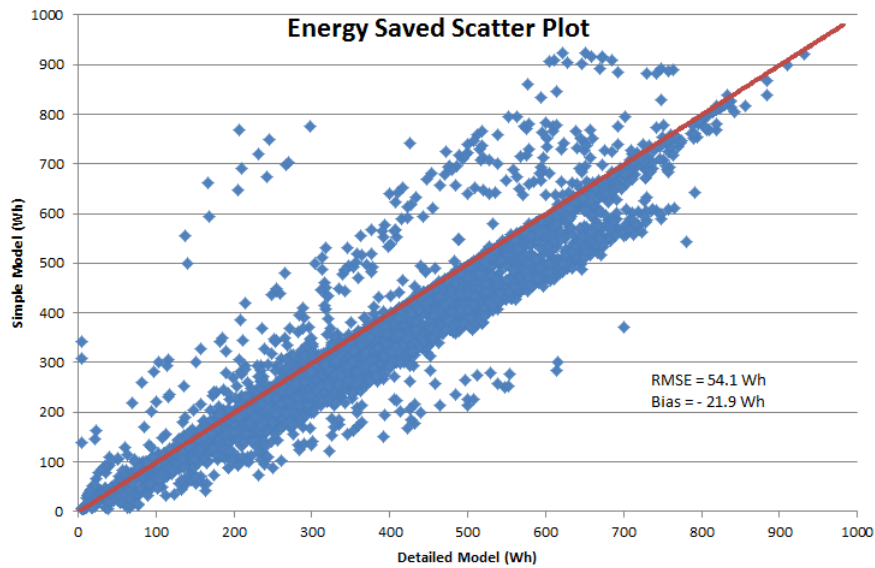


Figure 11. Scatter Plot

It is apparent that all values compared are within 10%, providing validation that the simple model estimates reasonable values for annual performance quantities of interest.

6 Transitioning From SAM-TRNSYS

6.1 SAM-TRNSYS Model

To provide a transition pathway from the older solar water heating model in SAM, results will also be presented from SAM and discussed in the context of how the models differ. Previous users of SAM's solar water heating model have been using a two-tank glycol system. The first tank is the solar storage tank, while the second is an auxiliary electric tank. Users input properties of both tanks as well as any desired economic inputs, and then run the simulation. There is only one node in the solar tank, which can cause under-prediction of energy saved.

6.2 Motivation for replacement

There is interest in replacing the older SAM model with this simple model for two primary reasons. The first is to speed the calculation up, the second is to provide a more understandable system interface for the user. The primary problem with this model is not that the inputs are too difficult, but rather that many of the variables are hard-coded and not sufficiently explained in user documentation. This presents a problem when trying to compare models or modify the solar water heating system. Table 3 illustrates hard-coded values in the SAM-TRNSYS model.

The simple model allows the user to select the irradiance model, specify the ground reflectance (albedo), and collector mass flow rate. Users can also choose which components of the irradiation should be used to compute the incident irradiation. These inputs can have drastic influence on annual results; therefore, it seems reasonable that users should be given control over their values.

Table 3. Hard-Coded SAM-TRNSYS Values

Variable	Value
Albedo	0.2
Irradiance Model	Hayes Davies
Irradiance Inputs	Total and Beam
Collector \dot{m}	$55 \frac{kg}{m^2s}$

Finally, the simple model replaced the SAM-TRNSYS implementation to reduce computational cost. One of the appeals of SAM is that users can run parametric analysis to determine which system configurations, locations, and economic models provide them with the best way to go renewable; however, parametric simulations are only useful if they can be done in a reasonable amount of time. For this reason, TRNSYS is not the best tool for completing parametric simulations. Preliminary results suggest about a 10x speed-up using the simpler model.

6.3 Simple Model Comparison

Simulations were conducted using Denver International Airport as a common location, except for one parametric simulation using San Francisco, Phoenix, Wilmington (DE), Key West, and Des Moines. Values for the simple model were matches as close as possible to the hard-coded values from Table 3. Other values that were modified from Table 1 when comparing the simple model to SAM-TRNSYS are listed in Table 4.

Table 4. Simple to SAM comparison parameters

Variable	Value
Collector \dot{m}	$0.046 \frac{kg}{s}$
Collector Area	$2.98 m^2$
$F_R(\tau\alpha)$	0.689
$F_R U_L$	$3.85 \frac{W}{m^2C}$

6.3.1 Tank Temperature

Figure 12 shows the daily averaged tank temperatures.

It appears that the simple dual-mode model predicts a higher average tank temperature than the SAM-TRNSYS model.

6.3.2 Energy Saved

A parametric analysis on the energy saved for the simple model produced the stacked bar charts in Figures 14 and 15. The figures illustrates trends which would be expected, for instance, increased tank volume and collector area yield increased energy saved. The trends are the same and the magnitudes match well, which should give transitioning users confidence that they can expect similar annual results using the new model.

Figure 15 shows comparison of daily average profiles at Denver International Airport.

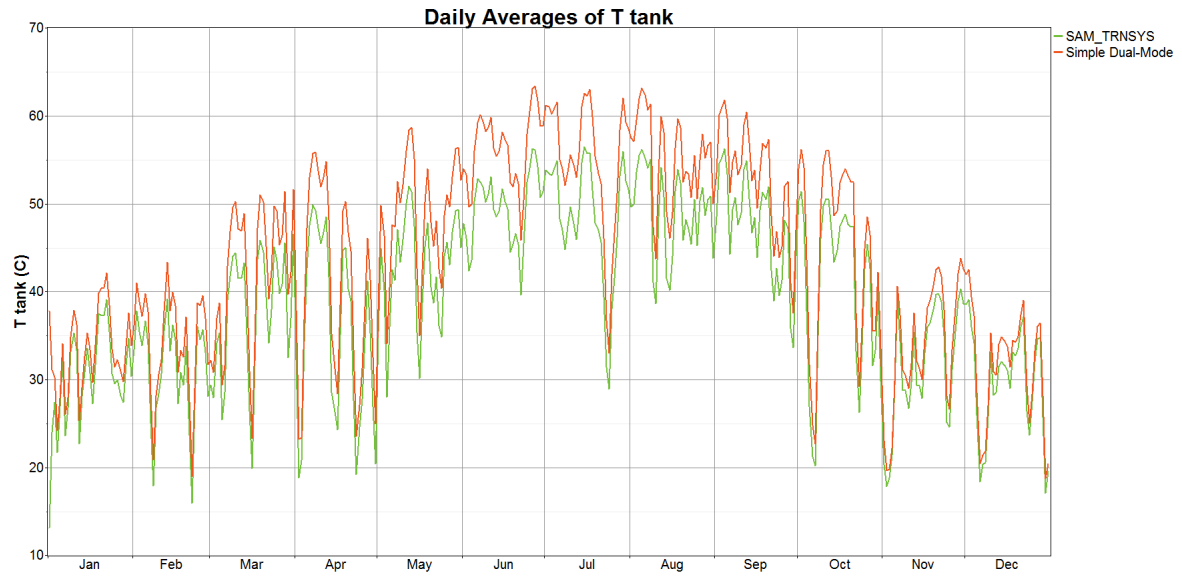


Figure 12. Comparison of Tank Temperatures

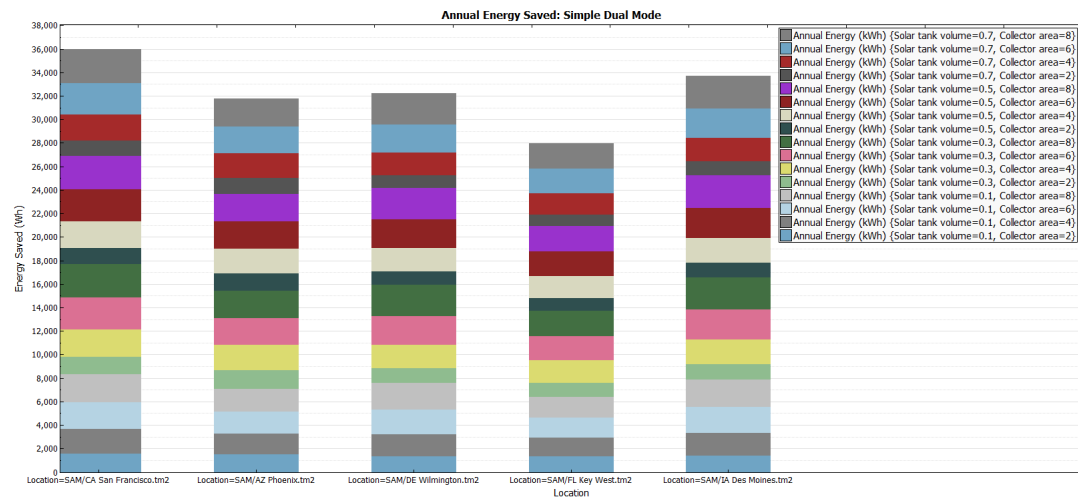


Figure 13. Dual Mode Parametric Analysis: Energy Saved

It appears that the daily average profiles are not exactly the same but follow the same general trend. Most importantly, while deviations exist in the predictions from hour to hour throughout the day, the total annual energy saved is similar.

6.3.3 Annual Percent Differences

Finally, it is instructive to consider the annual percent differences in various variables between the dual-mode model and SAM-TRNSYS, where the percent difference is calculated as:

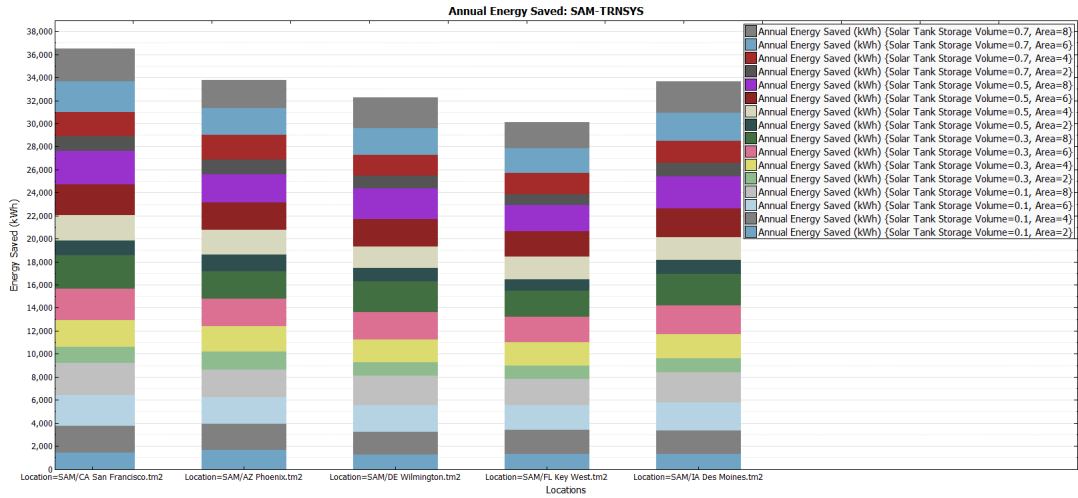


Figure 14. SAM Parametric Analysis: Energy Saved

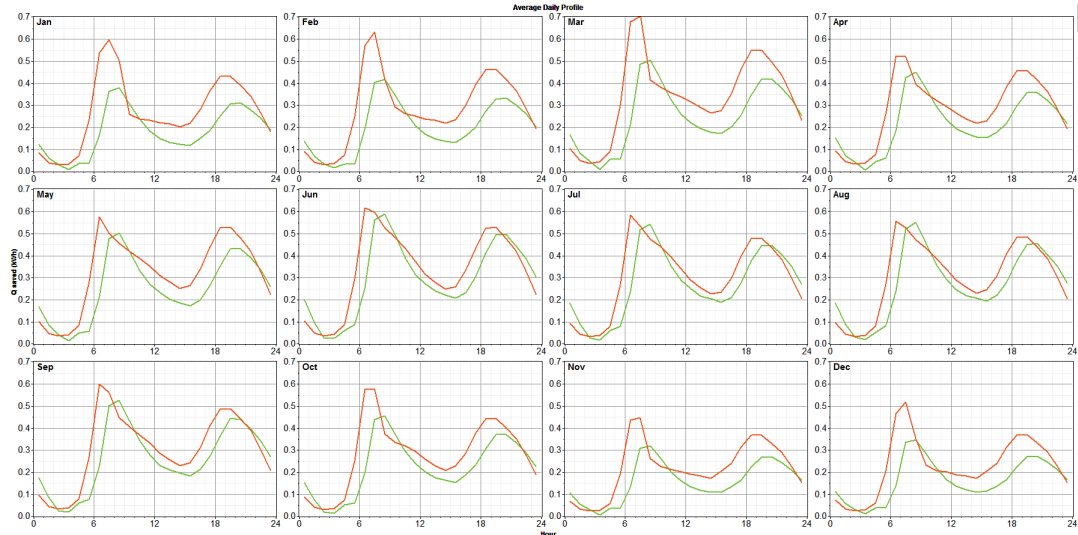


Figure 15. Typical Day Profile: Green = SAM-TRNSYS, Red = Simple Dual Mode

$$p = \frac{ST - Simple}{ST} * 100 \tag{6.3.1}$$

Where ST stands for SAM-TRNSYS. This equation allows for determination of whether the simple model over-predicts or under-predicts the SAM-TRNSYS result. Results for predicted percent differences of incident irradiance, useful collected energy, auxiliary energy required, and energy saved are shown in Table 5.

Energy saved is within $\pm 10\%$, while the auxiliary energy required to bring the water to the set temperature using solar water heating generally higher using SAM-TRNSYS.

Table 5. Annual Percent Differences

Location	Irradiance	Collected Energy	Aux. Energy	Energy Saved
Des Moines	0.53	-3.21	7.61	-3.54
Key West	0.20	-2.82	10.6	3.42
Phoenix	-0.88	-9.51	10.6	2.75
San Francisco	0.38	-3.84	11.49	-3.63
Wilmington	0.36	-3.52	2.42	-3.29

7 Conclusion

The differential equation governing the change in hot, cold, and mean tank temperatures were derived by performing a control volume energy analysis. All differential equations were approximated using the first-order accurate implicit Euler method. The methods tracked the same temperature and energy trends as a detailed TRNSYS simulation developed for validation. Future work could add sub-hourly calculations to better track transitions between modes. Additionally, a conduction model could be added to model heat transfer between nodes.

The simple two-mode model was also compared against an old model implemented in the System Advisor Model. The simple model predicted energy savings similar to SAM simulation. Parametric results were presented to give users confidence that the two models predict similar annual energy savings across a variety of system configurations and locations.

8 Nomenclature

Subscripts	
c	collector
e	exit
i	inlet
o	outside
p	previous hour
r	room
t	water storage tank
$cold$	cold node
$draw$	user draw
hot	hot node
$loss$	a computed energy loss
$mains$	from supply water
$useful$	adjusted for loss

Variables		
C_p	Specific Heat	J/kg-C
Δt	Time Step	s
h	Enthalpy	J/kg
H	Height	m
\dot{m}	Flow Rate	kg/s
ρ	Density	kg/m ³
T	Temperature	C
U	Loss Coefficient	W/C-m ²
A	Area	m ²
V	Volume	m ³

References

- [1] Klein, S., "TRNSYS: A Transient System Simulation Program: User's Manual, Version 16," 2006.
- [2] Christensen, C., B. J., "A Simplified Solar Water Heater Model with a Dual Mode Tank," *Draft*, 2013.
- [3] Burch, J.; Christensen, C., "Towards Development of an Algorithm for Mains Water Temperature," *Conference: Proceedings of the Solar 2007 Conference, 8-12 July 2007, Cleveland, Ohio (CD-ROM); Including Proceedings of 36th ASES Annual Conference, Proceedings of 32nd National Passive Solar Conference, and Proceedings of the 2nd Renewable Energy Policy and Marketing Conference*, 2007.
- [4] Scheffler, "Energy Balance For Variable Volume Storage," *Solar Energy*, Vol. 38, No. 1, 1987, pp. 9–10.
- [5] Duffie, J; Beckman, W., *Solar Engineering of Thermal Processes*, John Wiley and Sons, 3rd ed., 2006.

- [6] Moran, M; Shapiro, H., *Introduction to Thermal Systems Engineering: Thermodynamics, Fluid Mechanics, and Heat Transfer*, John Wiley and Sons, 5th ed., 2002.
- [7] Burden, R; Faires, J., *Numerical Analysis*, Brooks-Cole, 9th ed., 2010.
- [8] Reindl, D Beckman, W. D. J., "Evaluation of Hourly Tilted Surface Radiation Models," *Solar Energy*, Vol. 45, No. 9, 1990.
- [9] Perez, R. Ineichen, S. R. M. J. S. R., "Modeling Daylight Availability and Irradiance Components from Direct and Global Irradiance," *Solar Energy*, Vol. 44, No. 271, 1990.